The Journal of Experimental Biology 205, 3425–3433 (2002)
Printed in Great Britain © The Company of Biologists Limited 2002
JEB4345



# The eyes of suckermouth armoured catfish (Loricariidae, subfamily Hypostomus): pupil response, lenticular longitudinal spherical aberration and retinal topography

Ron H. Douglas[1,*], Shaun P. Collin[2,3] and Julie Corrigan[1]

[1]*Applied Vision Research Centre, Department of Optometry & Visual Science, City University, Northampton Square, London EC1V 0HB, UK,* [2]*Department of Anatomy & Developmental Science, School of Biomedical Science, The University of Queensland, Brisbane 4072, Queensland, Australia* and [3]*Anatomisches Institut, Universität Tübingen, Österbergstrasse 3, Tübingen, 72074, Germany*

*Author for correspondence (e-mail: r.h.douglas@city.ac.uk)

*Accepted 8 August 2002*

## Summary

**The dilated, round pupils of a species of suckermouth armoured catfish (*Liposarcus pardalis*) constrict slowly on illumination (over 35–40 min) to form crescent-shaped apertures. Ray tracing of He–Ne laser beams shows that the lenses of a related species (*Pterygoplichthys etentaculus*), which also has a crescent-shaped pupil, are well corrected for longitudinal spherical aberration, suggesting that the primary purpose of the irregular pupil in armoured catfish is not to correct such aberration. It is suggested that the iris operculum may serve to camouflage the pupil of these substrate-dwelling species. An examination of the catfish retina shows the photoreceptors to be exclusively single cones interspersed with elongate rods and demonstrates the presence of multiple optic nerve head papillae. Two areas of high ganglion cell density, each side of a vertically oriented falciform process, provide increased spatial resolving power along the axes examining the substrate in front of and behind the animal.**

Key words: catfish, pupil, retina, iris, aberration, *Liposarcus pardalis*, *Pterygoplichthys etentaculus*.

## Introduction

The pupil of the majority of teleost fish, unlike in most other vertebrates, does not change in size in response to variation in ambient illumination, and the iris is generally assumed to be immobile. However, a review of earlier literature shows that some teleosts are, in fact, able to change the size of their pupil quite considerably, and recently we provided the first quantitative assessment of such changes in fish, describing pupillary mobility in the marine plainfin midshipman *Porichthys notatus* that was as rapid and extensive as that in humans (Douglas et al., 1998).

The aim of the present study was to quantify the pupil responses of another group of teleosts; the suckermouth armoured catfish, which belong to the Loricariid family of Siluriform catfish resident in the freshwaters of Panama and South America. Specifically, we investigated members of the subfamily Hypostomus, which, along with some other members of the Loricariidae, are popularly referred to by the generic name ‘Pleco’ or ‘Plecostomus’, but, in fact, comprise over 100 species in approximately 18 genera (Nelson, 1994). This group was chosen for study because Walls (1963) suggested that they may show extensive pupil mobility, although no details of the extent and speed of migration were provided. Clearly, however, the pupil responses of these catfish will be very different to those of *P. notatus*, because although the fully dilated pupil is, as in most other vertebrates, round, when constricted it takes on the shape of a ‘crescent moon’ owing to the presence of a dorsal iris operculum.

Iris opercula are common among some elasmobranch fish, such as skates and batoid rays (Beer, 1894; Franz, 1905, 1931; Young, 1933; Walls, 1963; Kuchnow and Martin, 1970; Kuchnow, 1971; Gruber and Cohen, 1978; Nicol, 1978; Collin, 1988), and also occur in some bottom-dwelling teleosts (Bateson, 1890; Beer, 1894; Walls, 1963; Munk, 1970; Collin and Pettigrew, 1988a; Nicol, 1989). Despite the relatively widespread occurrence of such asymmetric pupils, their function remains uncertain. One explanation is that they may reduce the effect of any longitudinal spherical aberration the lens might possess by restricting light to the lens periphery (Murphy and Howland, 1991). Most fish suffer little from longitudinal spherical aberration owing to a refractive index gradient within the lens (see Sivak, 1990 for a review). However, if crescent-shaped pupils do function primarily to reduce such aberration, one might expect the lenses of animals with these pupils to be poorly corrected for it. We therefore determined the longitudinal spherical aberration of the lens in a species of suckermouth armoured catfish.

Finally, the retinal ganglion cell topography of these catfish was assessed. Although few studies have investigated the density of retinal ganglion cells with crescent-shaped pupils, the crescent-shaped iso-density contours in retinal wholemounts of the sharp-nosed weaver *Parapercis cylindrica* (Teleostei; Collin and Pettigrew, 1988a) and the shovel-nosed ray *Rhinobatos batillum* (Elasmobranchii; Collin, 1988) in conjunction with a similarly shaped pupil suggest that a relationship may exist.

## Materials and methods

### *Animals*

All animals were obtained from local aquarium suppliers in London, UK and Tübingen, Germany and identified by the British Museum of Natural History, London.

### *Measurement of pupil response*

Three individual *Liposarcus pardalis* Castelnau 1855 [standard lengths (SL) 140–150 mm] were held in a 12 h:12 h L:D cycle for at least 3 months. To examine their pupil response, they were removed from their home tanks during the dark phase of their L:D cycle using a dim red torch and placed in a small aquarium. Following 1 h of acclimation to this tank, pupillary responses were filmed for 60 min using infrared illumination during continual exposure to one of 13 intensities of white light. Each fish was examined at the same time each day to avoid any circadian influences on the pupil response, receiving only one light exposure per day. As these animals naturally tend to stay motionless in the light, the only form of restraint necessary during filming was a Perspex 'tent' placed over them. Stimuli were delivered from directly overhead, via a shutter-controlled opening and a mirror, from a Kodak projector located in an adjacent room, which also housed all recording apparatus. The intensity of illumination was controlled by neutral density filters. One eye of each animal was videotaped using an infrared-sensitive camera (Cohu, San Diego, USA) positioned in a plane parallel to the cornea. Pupil area was subsequently determined from individual video frames using NIH-image. To facilitate comparison among individuals of different eye size, all measurements were expressed relative to the fully dilated pupil area of each animal just prior to experimental light exposure.

### *Determination of lens longitudinal spherical aberration*

Following immersion in a lethal dose of methane tricaine sulfonate salt (MS 222), both lenses were removed from a single *Pterygoplichthys etentaculus* Spix and Agassiz 1829 (SL 200 mm). *P. etentaculus*, whose pupil is also crescent shaped when constricted, was preferred to *L. pardalis* for this part of the study owing to its larger size. The lenses of *P. etentaculus*, which, like those of other suckermouth catfish (*L. pardalis*, *Glyptoperichthys lituratus* and *Sturisomatichthys* sp.; R. H. Douglas and S. P. Collin, unpublished data), are antero-posteriorly flattened, were glued to the tip of a fine pipette, placed in a small glass tank and immersed in a teleost Ringer solution containing small amounts of scatter liquid concentrate (Edmund Scientific, Barrington, USA). The beam of an He–Ne laser (emission maximum 632.8 nm) was then passed through the lens along the antero-posterior axes. A camera positioned at the side of the lens was used to ensure that the laser beam passed through its vertical midpoint. This was achieved by adjusting the height of the laser beam until it was not deflected by the lens from the horizontal plane. The laser beam was then filmed from above while traversing the lens in the horizontal plane. Individual video frames were analysed using software to determine the back vertex distance (BVD) for a number of beam entry positions. A non-linear regression was applied to the data using the following equation for back vertex distance ($x$): $x=a+by^2+cy^4$, where $a$ represents back vertex focal length, $b$ represents the 3rd order spherical aberration, $c$ represents the 5th order spherical aberration, and $y$ represents the normalised beam entry position. This equation represents the longitudinal ray aberration of a rotationally symmetric optical system on axis.

### *Retinal structure and ganglion cell topography*

The eyes of a single *L. pardalis* (SL 220 mm) were embedded in resin for light microscopy, and two interrupted series of 0.5 μm sections were cut on an ultramicrotome and stained with Toluidine Blue. One eye was serially sectioned in the dorso-ventral axis and the other along the naso-temporal axis.

Both eyes of two individuals of *Liposarcus multiradiatus* Hancock, 1828 (SL 88 mm) and one *L. pardalis* individual (SL 158 mm) were used for topographic analyses of retinal ganglion cell distribution. After 3 h of dark adaptation and immersion in a lethal dose of MS 222, eyes were enucleated with at least 2–3 mm of the optic nerve still attached. Extraocular muscle tissue was removed, with care taken not to puncture the eyecup. While immersed in oxygenated teleost Ringer solution, a further 1–2 mm of the optic nerve was removed, and the remaining nerve stump swabbed dry with a tissue wick. Crystals of fluorescein-conjugated dextran (3000 MW, anionic, lysine-fixable; Molecular Probes, Leiden, The Netherlands) were then applied to the entire diameter of the lesioned optic nerve. After approximately 5 min, to allow uptake of the dextran label, the whole eye was re-immersed in oxygenated Ringer solution for 24 h at 21°C.

Following incubation, the limbus of each eye was pierced and the cornea and lens were removed. A small dorsal incision was made in the retina for orientation. The eyecup was immersion fixed in 4% paraformaldehyde in 0.1 mol $l^{-1}$ phosphate buffer (pH 7.4) for 40 min before dissection in 0.1 mol $l^{-1}$ phosphate buffer. Each retina was removed from its scleral eyecup and wholemounted (ganglion cell layer uppermost) on a subbed slide (double-dipped in 5% gelatin), covered in either Fluoromount (Calbiochem, San Diego, USA) or 0.1 mol $l^{-1}$ phosphate buffer and coverslipped. Dehydration was inhibited by sealing the edges of the coverslip with nail polish. One retina of *L. multiradiatus* was wholemounted and prepared as above but left overnight in a humidified Petri dish

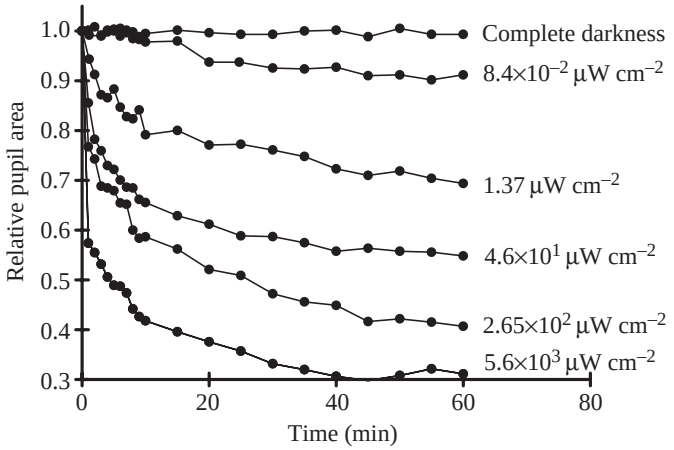


Fig. 1. Pupil response of a *Liposarcus pardalis* individual during 60 min exposure to different intensities of white light.

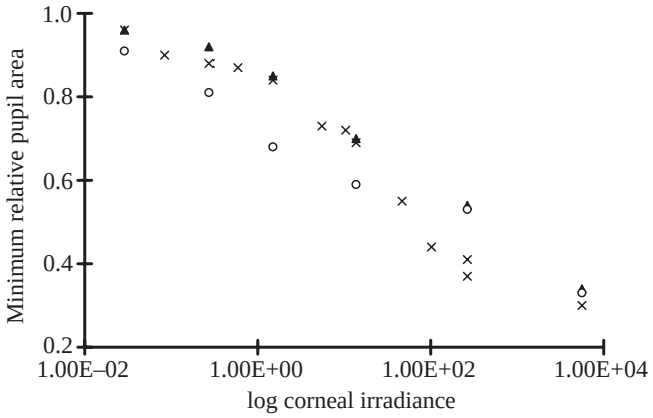


Fig. 2. Minimum pupil area in response to different intensities of white light. Corneal irradiance is measured in µW cm–2. The different symbols represent data from three individual *Liposarcus pardalis*.

before being stained for Nissl substance with 0.05% Cresyl Violet for 3 min. The wholemount was then dehydrated in a series of alcohols and mounted in DPX to reveal the distribution of glial cells.

Topographic analysis of the retrogradely labelled ganglion cells was carried out following the protocol of Collin and Northcutt (1993), where up to 200 regions per retina (50–60% of the retinal area) were sampled, allowing small fluctuations in density to be noted. Iso-density contours were constructed by joining areas of similar cell density. Retinal shrinkage was assumed to be minimal because all retinae were examined while hydrated. The total number of labelled ganglion cells was calculated by multiplying the average cell density between each iso-density contour by its area. Area measurements were calculated by scanning the topography map into a PC and analysing the area of each contour using NIH-Image. Retrogradely labelled ganglion cells were viewed and photographed on a Zeiss Axiophot 135M fluorescence microscope (Jena, Germany) fitted with a fluorescein filter block using Kodak Tmax 400 ASA film.

## Results

### *Pupil response*

Fig. 1 shows the pupil response of a single *L. pardalis* individual to six different intensities of illumination. The maximum amount of pupil constriction as a function of light intensity for all three *L. pardalis* examined is shown in Fig. 2. The threshold to elicit a measurable pupil response lies between a corneal irradiance of $2.9\times10^{-2}$ µW cm$^{-2}$ and $8.4\times10^{-2}$ µW cm$^{-2}$ for all animals. Overall, the response of the pupil to light was very slow. The time taken for half maximal contraction ($t_{0.5max}$) was in the order of 1–8 min, with full constriction usually taking 35–45 min. Once constricted, the pupil remained so for the duration of the experiment, showing no signs of re-dilating in continual illumination (Fig. 1).

Pupillary constriction in *L. pardalis* consists of two components; a general reduction in the diameter of the pupil and the outgrowth of an operculum from the dorsal margin of the iris (Fig. 3). Consequently, while the fully dilated pupil of *L. pardalis* is more or less round (Fig. 4A), when constricted it appears as a 'crescent moon' with an irideal flap obscuring the central pupil (Fig. 4B). In general, especially at higher light levels, the decrease in overall pupil diameter occurs more rapidly than the increase in opercular area (Fig. 3).

### *Longitudinal spherical aberration of the lens*

The lenses of *P. etentaculus* are well corrected for longitudinal spherical aberration, showing only relatively small differences in back vertex distance (BVD) for laser

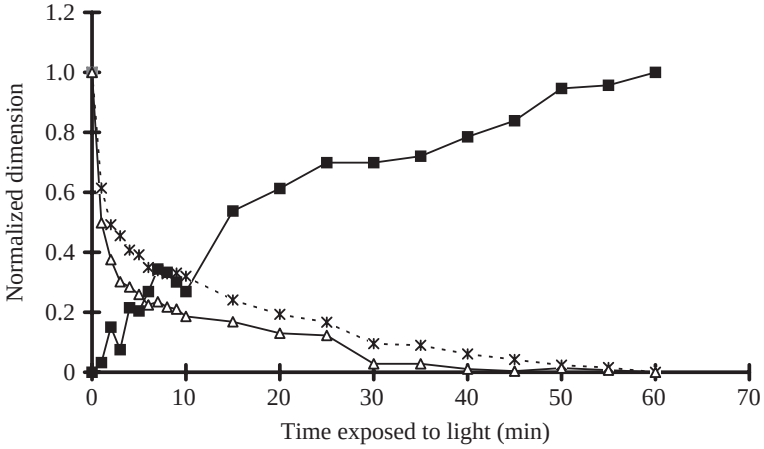


Fig. 3. Pupil response of a *Liposarcus pardalis* individual to 60 min exposure to white light at an intensity of $5.6\times10^{3}$ µW cm$^{-2}$. The three curves represent normalized lines for area of irideal operculum (squares), pupil area (crosses) and horizontal pupil diameter at its widest point (triangles).

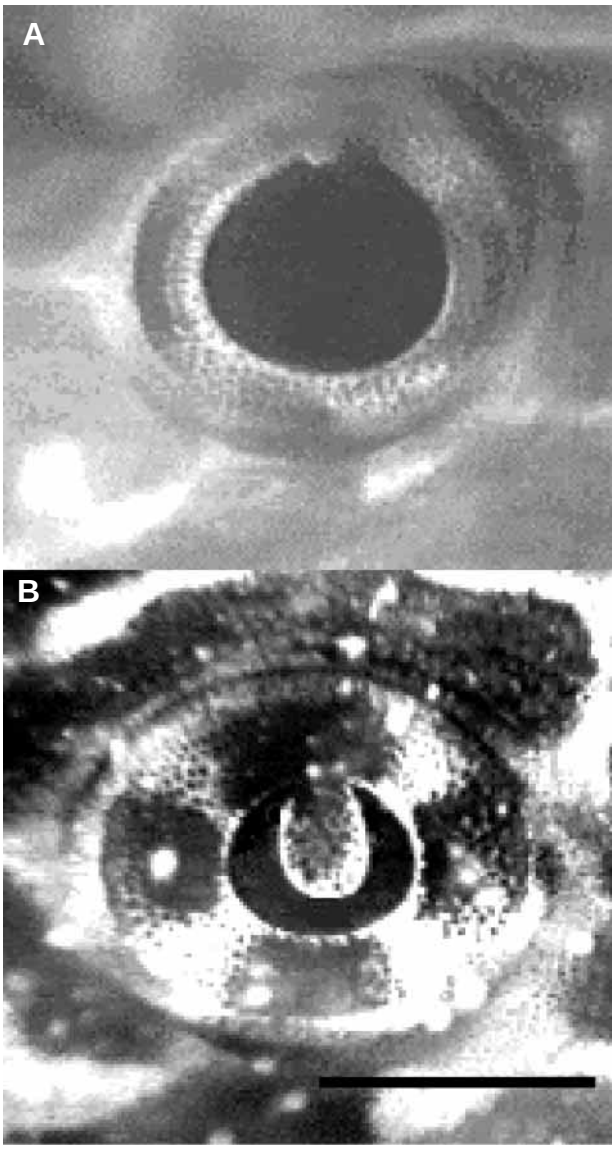


Fig. 4. Infra-red video images of the eye of *Liposarcus pardalis* (standard length 14 cm) in (A) the absence of any visible light and (B) after 60 min exposure to $5.6\times10^{3}\,\mu W\,cm^{-2}$ white light. Illumination resulted both in a decrease of pupil diameter and the outgrowth of an iris flap, such that overall pupil area following illumination in this example is 34% of the dark-adapted value. Scale bar, 2 mm.

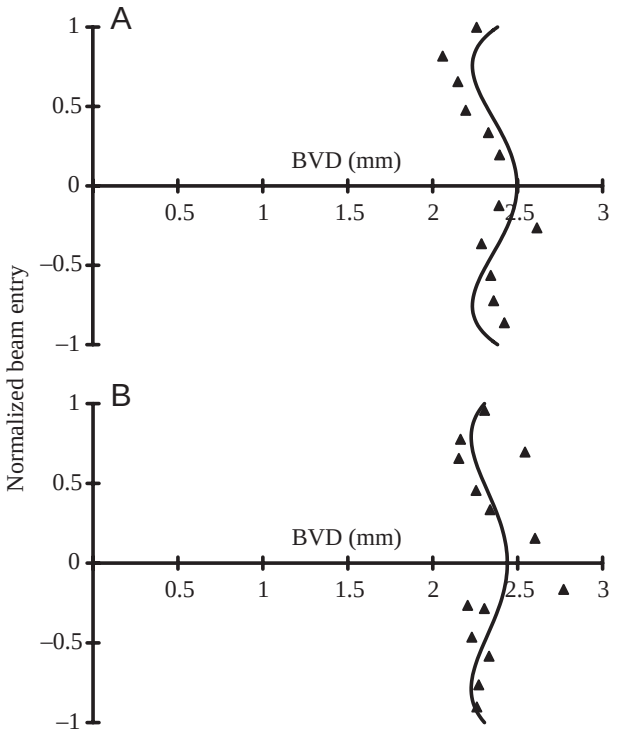


Fig. 5. Back vertex distance (BVD) as a function of entry position of an He–Ne laser beam into the (A) right (1.65 mm×1.88 mm diameter) and (B) left (1.63 mm×1.85 mm diameter) lens of a *Pterygoplichthys etentaculus* individual. The triangles represent individual data points, and the solid lines represent fitted non-linear regression lines [(A) $x=2.50–0.92y^{2}+0.80y^{4}$; (B) $x=2.44–0.68y^{2}+0.55y^{4}$]. The beam-entry positions have been normalised so that the edges of the lens represent 1 and –1.

beams passing through the lens at different points and displaying a balance between negative 3rd order and positive 5th order aberrations (Fig. 5). The maximum difference in BVD for beams passing through the lens at different points within the lens is approximately 10% of the total focal length.

### *Retinal structure*

In the isolated eyecup of all the various species of armoured catfishes examined, an elongated embryonic fissure extends from the central retina to the ventral margin. The choroid protrudes through the fissure to form a falciform process, which gives rise to an extensive system of vitreal blood vessels. In radial sections examined by light microscopy, the photoreceptors of the *L. pardalis* retina are exclusively single cones interspersed with elongate rods (Fig. 6).

### *Multiple optic nerve head papillae*

Histological sections cut parallel to the embryonic fissure reveal several discrete optic discs (papillae) running along the fissure. Ganglion cell axons backfilled with fluorescein-conjugated dextran, which are dispersed relatively evenly in peripheral retina, form discrete bundles or ‘fascicles’ as they approach the embryonic fissure (Figs 7A–C, 8). The thickness of each fascicle varies from 12 μm to 80 μm in diameter (Fig. 7D), and up to six fascicles may converge to form a single optic papilla (Fig. 7A,B). The optic nerve head, therefore, comprises a series of optic papillae, each fascicle converging from either unilateral or bilateral regions of the retina. At the dorsal end of the optic nerve head, the fascicles converge from temporal, dorsal and nasal retinal regions. Although predominantly located in the ganglion cell layer and separated from the optic fascicles, the retinal ganglion cells form loosely distributed columns lying between each optic fascicle (Fig. 8). In Cresyl Violet-labelled retinae, well-defined glial columns

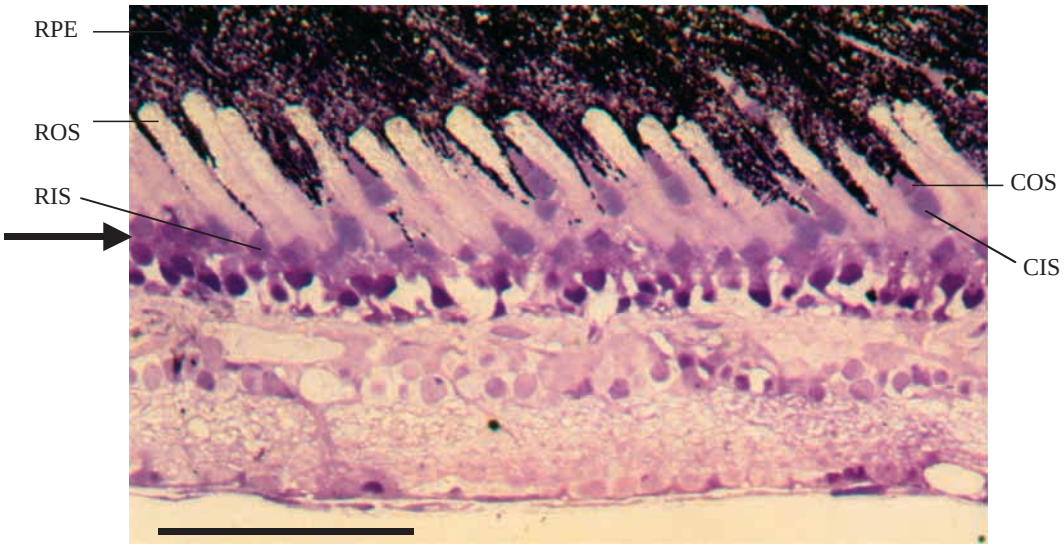


Fig. 6. Transverse section of a *Liposarcus pardalis* retina. The arrow indicates the position of the external limiting membrane. The only photoreceptors seen throughout the retina are large rods and small single cones. Abbreviations: RPE, retinal pigment epithelium; ROS, rod outer segment; RIS, rod inner segment; COS, cone outer segment; CIS, cone inner segment. Scale bar, 50 μm.

also emanate from the elongated series of optic nerve heads like the spokes of a wheel.

*Retinal ganglion cell topography*

Retrogradely labelled ganglion cells are distributed non-uniformly throughout the retina. Peaks in ganglion cell density, or *areae centrales*, lie on each side of the vertically oriented falciform process, just dorsal of the horizontal meridian. In *L. pardalis*, densities peak at $18.6\times10^2$ cells mm$^{-2}$ and $24.2\times10^2$ cells mm$^{-2}$ in nasal and temporal retinal regions, respectively (Fig. 9). In *L. multiradiatus*, densities are similar, with $18.6\times10^2$ cells mm$^{-2}$ and $16.4\times10^2$ cells mm$^{-2}$ in nasal and temporal retinal regions, respectively. Although not analysed topographically, a small population of displaced ganglion cells that lie in the inner nuclear layer were also labelled with a peak density of $2.5\times10^2$ cells mm$^{-2}$ in *L. multiradiatus*. The total number of retinal ganglion cells that lie either within the ganglion cell layer or within the inner nuclear layer in *L. pardalis* is 33 000.

## Discussion

*Dynamics of the pupil response*

The data indicate that armoured catfish are capable of extensive changes in pupil size that are directly related to the level of illumination, constricting to approximately 30% of their dark-adapted area in response to the highest light levels used (Figs 1, 2). While these migrations are extensive, they are not as great as those shown in comparable light levels by *P. notatus*, the only other teleost whose pupil response has been characterised in the same detail (Douglas et al., 1998). Furthermore, unlike in *P. notatus*, where pupil constriction in response to light is immediately followed by a redilation despite the continued presence of light, in *L. pardalis*, as in some nocturnal elasmobranchs (Kuchnow, 1971; Douglas et al., 1998), the pupil showed no signs of such a redilation.

However, the greatest difference between the pupil response dynamics of *P. notatus* and *L. pardalis* is in the speed of migration. As in humans and many other vertebrates, the $t_{0.5max}$ in *P. notatus* occurs in less than one second, while in *L. pardalis* the $t_{0.5max}$ is in the order of several minutes, with full constriction usually taking 35–45 min. The responses recorded here for *L. pardalis* are again similar in their time course to those observed in nocturnal elasmobranchs (Kuchnow, 1971; Douglas et al., 1998).

*Function of pupil closure*

In most lenses, light rays entering at different eccentricities will be focused at different distances behind the lens, inevitably blurring the image on the retina. In most terrestrial animals, the effects of longitudinal spherical aberration within the lens are minimised, as the cornea is the major refractive surface and the pupil can constrict to limit passage of light to only part of the lens. Lens quality, although important to any visual animal, is much more an issue for fish, as the cornea is effectively neutralised underwater, resulting in the lens being the only refractive surface, and in most species the lens protrudes through an immobile pupil with the whole lens consequently being involved in image formation. The degree of longitudinal spherical aberration recorded for fish lenses varies between species and with the age of the animal (Sivak, 1990). However, not surprisingly, the lens is generally well corrected for such aberration through the possession of a refractive index gradient (Sroczynski, 1976, 1978, 1979, 1981; Sivak and Kreuzer, 1983; Fernald and Wright, 1983; Kreuzer and Sivak, 1984; Jagger, 1992; Kröger and Campbell, 1996; Kröger et al., 1994, 2001; Garner et al., 2001). The degree of aberration observed here for the catfish is comparable with that recorded for other fish with immobile pupils. This suggests that it is unlikely that the main purpose of the mobile crescent-shaped pupil is to decrease the effects of longitudinal spherical aberration. This is in line with the observation reported for the clearnose skate *Raja elanteria*, which also has a crescent-

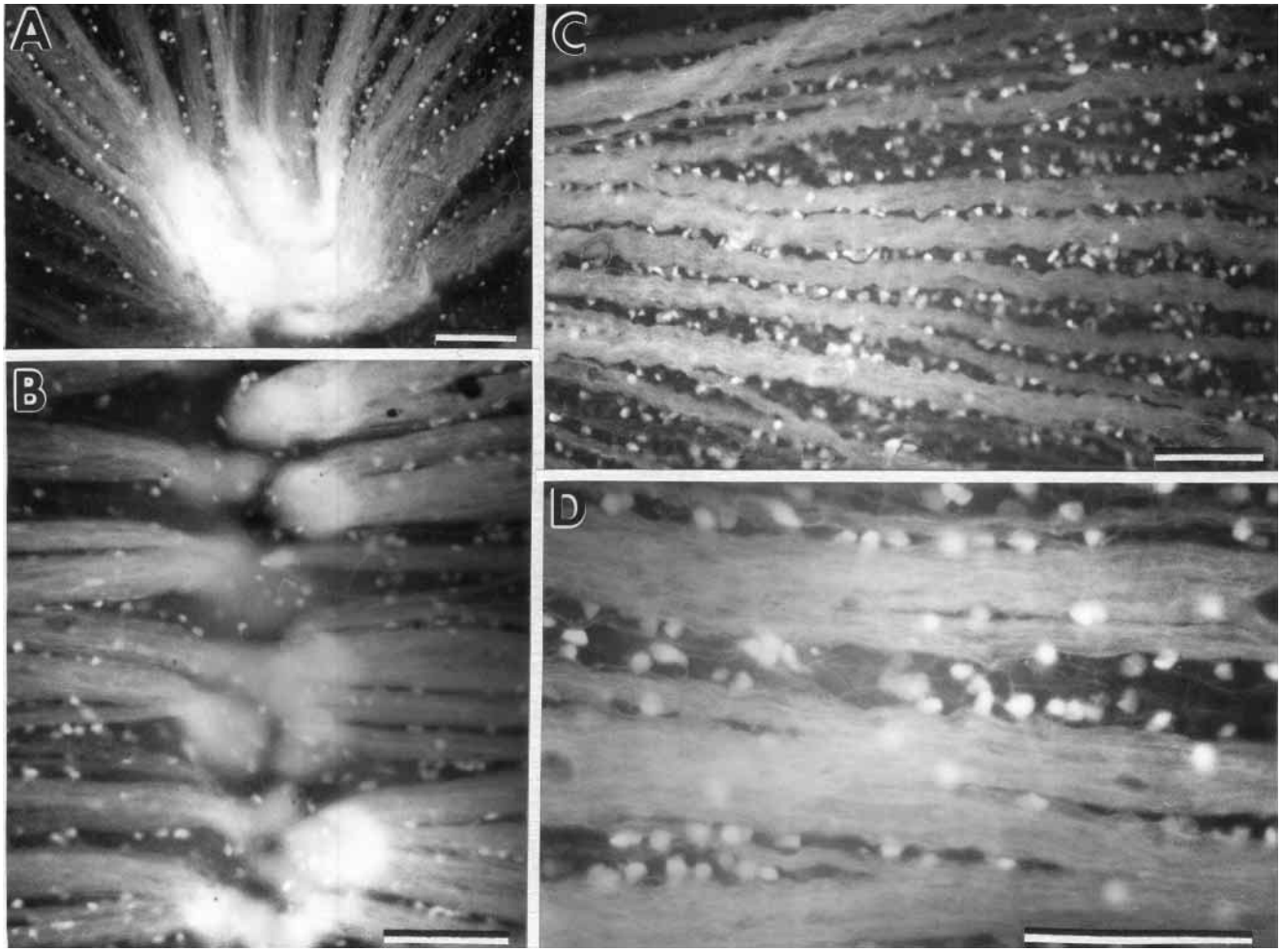


Fig. 7. Optic axon fasciculation. Ganglion cell axon fascicles labelled with fluorescein-tagged dextran (A) entering the dorsal region of the optic nerve head and (B) along the embryonic fissure in the retina of *Liposarcus multiradiatus*. (C) Low- and (D) high-power micrographs of retrogradely labelled ganglion cells lying in between axon fascicles. The embryonic fissure lies to the left in (C). Scale bars, 100 μm.

shaped pupil yet displays very little longitudinal spherical aberration (Sivak, 1991; Sivak and Luer, 1991).

We have previously suggested that, since the majority of teleost fish with extensive pupil mobility are bottom-dwelling animals that attempt to blend in with the substrate, the constriction of the pupil may aid in camouflaging the animal through obscuring the otherwise very visible pupil (Douglas et al., 1998). The same argument could be applied to *L. pardalis* and other bottom-dwelling suckermouth catfish, as the irideal operculum distorts the shape of the eye and blends with the rest of the fish's body markings when viewed by potential predators from above. The animal would, however, be able to maintain vision through its crescent-shaped pupil in the anterior, posterior and ventral directions, with two areas of increased acuity examining the substrate in front of and behind the animal (see below).

### *Retinal morphology*

In agreement with other studies on catfish (Ali and Anctil, 1976; Nicol, 1989; Pavan, 1946; Wagner, 1970; Ali and Wagner, 1975; Verrier, 1927, 1928; Douglas and Wagner, 1984; Nag and Sur, 1992; Sillman et al., 1993), the retina of *L. pardalis* is composed of single cones and large rods (Fig. 6). Double cones, which are present in most teleosts, appear to be absent from these species. This is surprising, as catfish often inhabit what could be classed as low-light-level environments and might therefore be expected to have retinae 'designed for sensitivity'. Thus, many catfish, for instance, have a retinal tapetum lucidum, a feature thought to enhance photon capture (Nicol et al., 1973; Arnott et al., 1974). There is evidence that double cones are a further mechanism for enhancing sensitivity. Ontogenetic development of double cones, for instance, is often associated with a change in lifestyle from brightly lit surface waters to inhabiting dimmer, deeper waters (e.g. Boehlert, 1978), and psychophysical experiments in birds suggest that double cones code for luminosity rather than being involved in colour vision (Maier and Bowmaker, 1993). Thus, one might expect large numbers of double cones in catfish

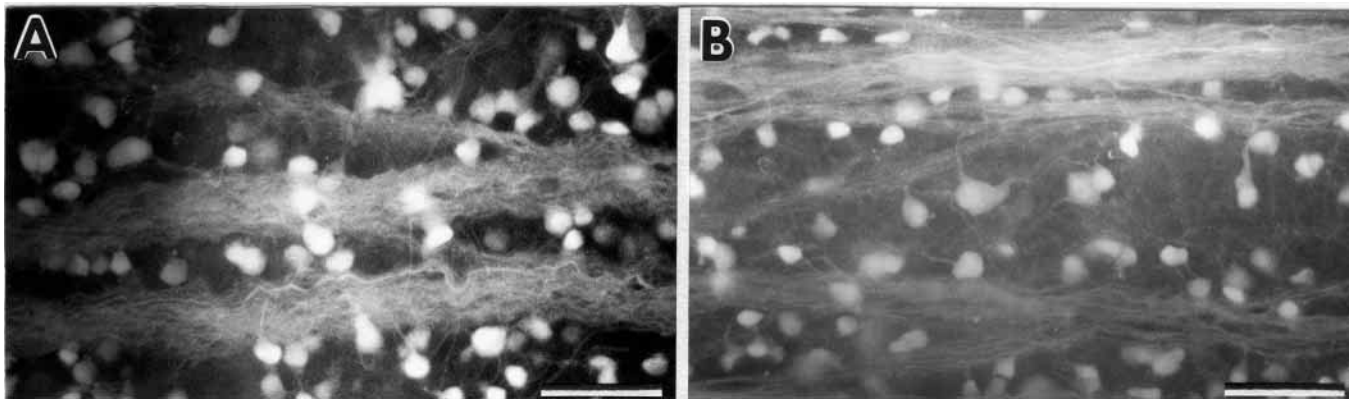


Fig. 8. Retinal ganglion cell labelling. (A,B) Retrogradely labelled retinal ganglion cells in the relatively high-density regions of the retina in *Liposarcus multiradiatus*. Note the heterogeneous cell soma size. Scale bars, 50 μm.

rather than their complete absence. However, there is circumstantial evidence that double cones are involved in movement detection in both birds (Campenhausen and Kirschfeld, 1998) and fish (Levine and MacNichol, 1982), especially when arranged in a square mosaic (Collin and Collin, 1999). The propensity of catfish to feed on non-mobile prey in generally turbid water may account for the lack of double cones. Alternatively, double cones seem to have a role in mediating polarisation sensitivity (Hawryshyn, 2000), an ability that catfish might therefore not possess.

As in members of most catfish families (Deyl, 1895; Ströer, 1939; Herrick, 1941; Wagner, 1970; Arnott et al., 1974; Ali and Anctil, 1976; Wagner et al., 1976; Frank and Goldberg, 1983, Dunn-Meynell and Sharma, 1987; Nag and Sur, 1992), the retinal ganglion cell axons of suckermouth catfish form discrete fascicles within the nerve fibre layer, leading to multiple optic papillae. The functional significance of this arrangement is unknown but a number of theories have been presented to explain the existence of multiple nerve heads in catfish. These include reducing the size of a large scotoma into several smaller scotomata (Walls, 1963; Dunn-Meynell and Sharma, 1987), reducing image degradation, which may be evident as light travels through the thick layers of optic fibres near a large optic nerve head (Wagner, 1970), and enhancing stimulus perception (Walls, 1963). Although breaking up the large scotoma resulting from a single papilla into small, less-obtrusive scotomata may be advantageous, the fact that the optic papillae in *L. pardalis* are not dispersed as in other catfish (e.g. the channel catfish *Ictalurus punctatus*; Dunn-Meynell and Sharma, 1987) suggests that this novel arrangement is associated with the topographic order of axons as they enter the optic nerve (Dunn-Meynell and Sharma, 1988).

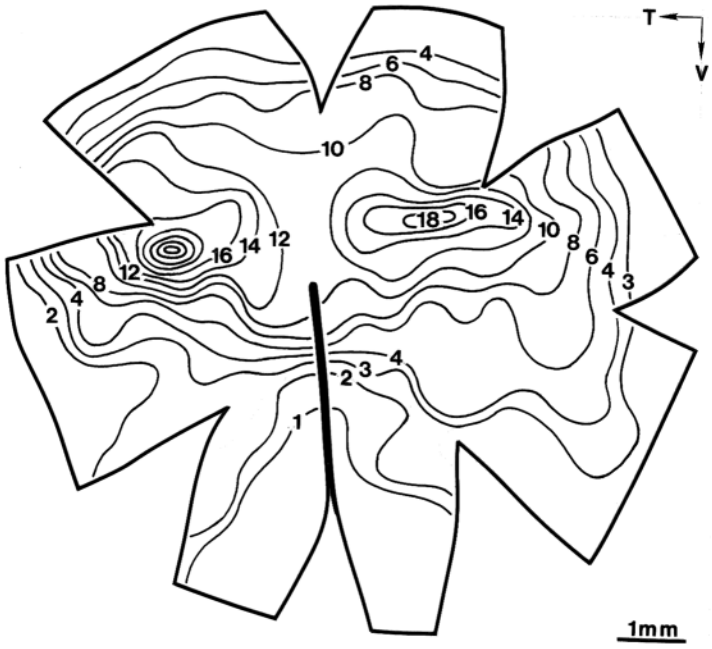


Fig. 9. Iso-density contour map of the distribution of retrogradely labelled retinal ganglion cells in the right eye of *Liposarcus pardalis* (standard length 158 mm). The elongated optic nerve head is depicted in black. All densities are $\times 10^2$ cells mm$^{-2}$. T, temporal; V, ventral.

### *Retinal topography*

A variety of patterns of peaks in retinal ganglion cell density have been found in a range of teleosts (Ito and Murakami, 1984; Collin and Pettigrew, 1988a,b; Collin, 1999) and elasmobranchs (Hueter, 1991; Collin, 1988; Bozzano and Collin, 2000). The nasal and temporal *areae centrales* in *L. pardalis* and *L. multiradiatus* would provide increased sampling, and therefore increased spatial resolving power, in the rostro-ventral and caudo-ventral axes, respectively. The arrangement of iso-density contours broadly follows the shape of the pupil, where the retinal region underlying the operculum possesses relatively low densities of ganglion cells, creating a high centro-peripheral density gradient of more than 25:1 (Fig. 9). Similarly, the lack of a dorsal pupillary operculum is also reflected in the topographic distribution of retinal ganglion cells in *I.*

*punctatus*. Using horseradish peroxidase as a retrograde tracer from the optic nerve, Dunn-Meynell and Sharma (1987) revealed a naso-temporal elongation of iso-density contours with a continuous peak of $>1.5\times10^2$ cells $mm^{-2}$ lying across the dorsal hemifield. The decrease in ganglion cell density underlying the operculum in *L. pardalis* is not present, which is indicative of an increased dependence on scanning a wider panoramic visual field in *I. punctatus*. A similar relationship to that seen in *L. pardalis* occurs in the eyes of the sharp-nosed weaverfish *Parapercis cylindrica* (Collin and Pettigrew, 1988a) and the shovel-nosed ray *Rhinobatos batillum* (Collin, 1988), where the shape of a crescent-shaped pupil is reflected in the distribution of ganglion cells, with two *areae* divided by a region of low density. Interestingly, the pupils of many cetacea (Kröger and Kirschfeld, 1993) and some elasmobranchs (Douglas et al., 1998) close down to two roughly horizontally aligned pinholes, and both of these groups also often have two retinal areas of maximal resolution (cetacea – Dral, 1983; Mass and Supin, 1995; Murayama et al., 1995; Murayama and Somiya, 1998: elasmobranchs – Peterson and Rowe, 1980; Bozzano and Collin, 2000; Collin, 1999).

However, it is in many ways surprising to find such similarity between ganglion cell distribution and pupil shape, as the pupil functions as an aperture stop and not a field stop. So it is perhaps not unexpected that a similar topographic regionalisation of the retina into two *areae* is found in a number of elasmobranchs (Peterson and Rowe, 1980; Bozzano and Collin, 2000; Collin, 1999; L. Litherland and S. P. Collin, unpublished data) that appear not to have a pupillary operculum or double pinhole apertures, suggesting that the need to optimise acuity in the frontal and caudal visual axes may be the driving force behind the development of retinal cell gradients rather than the presence of an irregular pupil.

The authors are grateful to Darrell Siebert (British Museum of Natural History), Michael Hardman (University of Illinois) and Nigel Merrett (British Museum of Natural History) for identification of specimens and to Christine Wood for the gift of one of the animals. Thanks also to Minal Patel for assistance with light microscopy, Paul Dyer for performing some preliminary pupillometry, Manesh Patel for help in determining lens aberrations and Jochen Wagner for providing the facilities for the topographic studies. Special thanks go to Ronald Kröger for designing the software used to analyse lenticular spherical aberration and to Chris Hull for fitting curves to the data. Dan-Eric Nilsson gave helpful comments on an earlier version of the manuscript. Part of this work was funded by a bursary from the Nuffield Foundation to R.H.D. S.P.C. was funded by the Alexander von Humboldt Stiftung while in Germany and an ARC QE II Research Fellowship in Australia.

## References

**Ali, M. A. and Anctil, M.** (1976). *Retinas of Fishes: An Atlas*. Berlin: Springer Verlag.

**Ali, M. A. and Wagner, H.-J.** (1975). Visual pigments; phylogeny and ecology. In *Vision in Fishes: New Approaches in Research* (ed. M. A. Ali), pp. 481-516. New York: Plenum Press.

**Arnott, H. J., Best, A. C. G. and Nicol, J. A. C.** (1974). Studies on the eyes of catfishes with special reference to the tapetum lucidum. *Proc. R. Soc. Lond. B Biol. Sci.* **186**, 13-36.

**Bateson, W.** (1890). Contractility of the iris in fishes and cephalopods. *J. Mar. Biol. Assoc. UK* **1**, 215-216.

**Beer, T.** (1894). Die Akkommodation des Fischauges. *Pflügers Arch. Ges. Physiol.* **58**, 523-650.

**Boehlert, G. W.** (1978). Intraspecific evidence for the function of single and double cones in the teleost retina. *Science* **202**, 309-311.

**Bozzano, A. and Collin, S. P.** (2000). Retinal ganglion cell topography in elasmobranchs. *Brain Behav. Evol.* **55**, 191-208.

**Campenhausen, M. V. and Kirschfeld, K.** (1998). Spectral sensitivity of the accessory optic system of the pigeon. *J. Comp. Physiol.* A **183**, 1-6.

**Collin, S. P.** (1988). The retina of the shovel-nosed ray, *Rhinobatos batillum* (Rhinobatidae): morphology and quantitative analysis of the ganglion, amacrine and bipolar cell populations. *Exp. Biol.* **47**, 195-207.

**Collin, S. P.** (1999). Behavioural ecology and retinal cell topography. In *Adaptive Mechanisms in the Ecology of Vision* (ed. S. N. Archer, M. B. A. Djamgoz, E. R. Loew, J. C. Partridge, S. Vallerga), pp. 509-535. London: Kluwer Academic Publishers.

**Collin, S. P. and Collin, H. B.** (1999). The foveal photoreceptor mosaic in the pipefish, *Corythoichthyes paxtoni* (Syngnathidae, Teleostei). *Histol. Histopathol.* **14**, 369-382.

**Collin, S. P. and Northcutt, R. G.** (1993). The visual system of the Florida garfish, *Lepisosteus platyrhincus* (Ginglymodi): III. Retinal ganglion cells. *Brain Behav. Evol.* **42**, 295-320.

**Collin, S. P. and Pettigrew, J. D.** (1988a). Retinal topography in reef teleosts. I. Some species with well-developed areae but poorly-developed streaks. *Brain Behav. Evol.* **31**, 269-282.

**Collin, S. P. and Pettigrew, J. D.** (1988b). Retinal topography in reef teleosts. II. Some species with prominent horizontal streaks and high density areae. *Brain Behav. Evol.* **31**, 283-295.

**Deyl, J.** (1895). Über den Sehnerven bel siluroiden und acanthopsiden. *Anat. Anz.* **11**, 8-16.

**Douglas, R. H. and Wagner, H.-J.** (1984). Action spectra of photomechanical cone contraction in the catfish retina. *Invest. Ophthalmol. Vis. Sci.* **25**, 534-538.

**Douglas, R. H., Harper, R. D. and Case, J. F.** (1998). The pupil response of a teleost fish, *Porichthys notatus*: description and comparison to other species. *Vision Res.* **38**, 2697-2710.

**Dral, A. D. G.** (1983). The retinal ganglion cells of *Delphinus delphis* and their distribution. *Aquat. Mamm.* **10**, 57-68.

**Dunn-Meynell, A. A. and Sharma, S. C.** (1987). Visual system of the channel catfish (*Ictalurus punctatus*): II. The morphology associated with the multiple optic papillae and retinal ganglion cell distribution. *J. Comp. Neurol.* **257**, 166-175.

**Dunn-Meynell, A. A. and Sharma, S. C.** (1988). Visual system of the channel catfish (*Ictalurus punctatus*): III. Fibre order in the optic nerve and optic tract. *J. Comp. Neurol.* **268**, 299-312.

**Fernald, R. D. and Wright, S. E.** (1983). Maintenance of optical quality during crystalline lens growth. *Nature* **301**, 618-620.

**Frank, B. L. and Goldberg, S.** (1983). Multiple optic fiber patterns in the catfish retina. *Invest. Ophthalmol. Vis. Sci.* **24**, 1429-1432.

**Franz, V.** (1905). Zur Anatomie, Histologie und functionellen Gestaltung des Selachierauges. *Jenaische Zeitschrift für Naturwissenschaft* **40**, 697-840.

**Franz, V.** (1931). Die Akkommodation des Selachierauges und seine Abblendungsapparate, nebst Befunden an der Retina. *Zool. Jahrb. Abt. Allg. Zool. Physiol. Tiere* **49**, 323-462.

**Garner, L. F., Smith, G., Yao, S. and Augusteyn, R. C.** (2001). Gradient refractive index of the crystalline lens of the black oreo dory (*Allocyttus niger*): comparison of magnetic resonance imaging (MRI) and laser ray-trace methods. *Vision Res.* **41**, 973-979.

**Gruber, S. H. and Cohen, J. L.** (1978). Visual system of the elasmobranchs: state of the art 1960-1975. In *Sensory Biology of Sharks and Rays* (ed. E. S. Hodgson and R. F. Mathewson), pp. 11-105. Arlington, VA, USA: Office of Naval Research.

**Hawryshyn, C. W.** (2000). Ultraviolet polarization vision in fishes: possible mechanisms for coding e-vector. *Phil. Trans. Roy. Soc. Lond. B Biol. Sci.* **355**, 1187-1190.

**Herrick, C. J.** (1941). The eyes and optic paths of the catfish, *Ameiurus*. *J. Comp. Neurol.* **75**, 255-286.

**Hueter, R. E.** (1991). Adaptations for spatial vision in sharks. *J. Exp. Zool.* **5 Suppl.**, 130-141.
**Ito, H. and Murakami, T.** (1984). Retinal ganglion cells in two teleost species, *Sebasticus marmoratus* and *Navodon modestus*. *J. Comp. Neurol.* **229**, 80-96.
**Jagger, W. S.** (1992). The optics of the spherical fish lens. *Vision Res.* **32**, 1271-1284.
**Kreuzer, R. O. and Sivak, J. G.** (1984). Spherical aberration of the fish lens; interspecies variation and age. *J. Comp. Physiol. A* **154**, 415-422.
**Kröger, R. H. H. and Campbell, M. C. W.** (1996). Dispersion and longitudinal chromatic aberration of the crystalline lens of the African cichlid fish *Haplochromis burtoni*. *J. Opt. Soc. Am. A* **13**, 2341-2347.
**Kröger, R. H. H. and Kirschfeld, K.** (1993). Optics of the harbor porpoise eye in water.. *J. Opt. Soc. Am. A* **10**, 1481-1489.
**Kröger, R. H. H., Campbell, M. C. W., Munger, R. and Fernald, R. D.** (1994). Refractive index distribution and spherical aberration in the crystalline lens of the African cichlid fish, *Haplochromis burtoni*. *Vision Res.* **34**, 1815-1822.
**Kröger, R. H. H., Campbell, M. C. W. and Fernald, R. D.** (2001). The development of the crystalline lens is sensitive to visual input in the African cichlid fish, *Haplochromis burtoni*. *Vision Res.* **41**, 549-559.
**Kuchnow, K. P.** (1971). The elasmobranch pupillary response. *Vision Res.* **11**, 1395-1406.
**Kuchnow, K. P. and Martin, R.** (1970). Fine structure of elasmobranch iris muscle and associated nervous structures. *Exp. Eye Res.* **10**, 345-351.
**Levine, J. S. and MacNichol, E. F., Jr** (1982). Colour vision in fishes. *Sci. Am.* **246**, 108-117.
**Maier, E. J. and Bowmaker, J. K.** (1993). Colour vision in the passeriform bird, *Leiothrix lutea*: correlation of visual pigment absorbance and oil droplet transmission with spectral sensitivity. *J. Comp. Physiol. A* **172**, 295-301.
**Mass, A. M. and Supin, A. Y.** (1995). Ganglion cell topography of the retina in the bottlenosed dolphin, *Tursiops truncatus*. *Brain Behav. Evol.* **45**, 257-265.
**Munk, O.** (1970). On the occurrence and significance of horizontal band-shaped retinal areae in teleosts. *Vidensk. Medd. Dan. Naturhist. Foren. Khobenhavn* **133**, 85-120.
**Murayama, T. and Somiya, H.** (1998). Distribution of ganglion cells and object localizing ability in the retina of three cetaceans. *Fish. Sci.* **64**, 27-30.
**Murayama, T., Somiya, H., Aoki, I. and Ishii, T.** (1995). Retinal ganglion cell size and distribution predict visual capabilities of Dall's porpoise. *Mar. Mamm. Sci.* **11**, 136-149.
**Murphy, C. J. and Howland, H. C.** (1991). The functional significance of crescent-shaped pupils and multiple pupillary apertures. *J. Exp. Zool.* **5 Suppl.**, 22-28.
**Nag, T. C. and Sur, R. K.** (1992). Cones in the retina of the catfish, *Clarius batrachus* (L.). *J. Fish Biol.* **40**, 967-969.
**Nelson, J. S.** (1994). *Fishes of the World*. Third edition. New York: Wiley.
**Nicol, J. A. C.** (1978). Studies on the eye of the stingray *Dasyatis sabina*, with notes on other selachians. I. Eye dimensions, cornea, pupil and lens. *Contrib. Mar. Sci.* **21**, 89-102.
**Nicol, J. A. C.** (1989). *The Eyes of Fishes*. Oxford: Oxford University Press.
**Nicol, J. A. C., Arnott, H. J. and Best, A. C. G.** (1973). Tapeta lucida in bony fishes (Actinopterygii): a survey. *Can. J. Zool.* **51**, 69-81.
**Pavan, C.** (1946). Observations and experiments on the cavefish *Pimelodella kronei* and its relatives. *Am. Natural.* **80**, 343-361.
**Peterson, E. H. and Rowe, M. H.** (1980). Different regional specializations of neurons in the ganglion cell layer and inner plexiform layer of the California horned shark, *Heterodontus francisci*. *Brain Res.* **201**, 195-201.
**Sillman, A. J., Ronan, S. J. and Loew, E. R.** (1993). Scanning electron microscopy and microspectrophotometry of the photoreceptors of ictalurid catfishes. *J. Comp. Physiol. A* **173**, 801-807.
**Sivak, J. G.** (1990). Optic variability of the fish lens. In *The Visual System of Fish* (ed. R. H. Douglas and M. B. A. Djamgoz), pp. 63-80. London: Chapman & Hall.
**Sivak, J. G.** (1991). Elasmobranch visual optics. *J. Exp. Zool.* **5 Suppl.**, 13-21.
**Sivak, J. G. and Kreuzer, R. O.** (1983). Spherical aberration of the crystalline lens. *Vision Res.* **23**, 59-70.
**Sivak, J. G. and Luer, C. A.** (1991). Optical development of the ocular lens of an elasmobranch, *Raja elanteria*. *Vision Res.* **31**, 373-382.
**Sroczynski, S.** (1976). Die chromatische Aberration der Augenlinse der Regenbogenforelle (*Salmo gairdneri* RICH.). *Zool. Jahrb. Abt. Allg. Zool. Physiol. Tiere* **80**, 432-450.
**Sroczynski, S.** (1978). Die chromatische Aberration der Augenlinse der Bachforelle (*Salmo trutta fario* L.). *Zool. Jahrb. Abt. Allg. Zool. Physiol. Tiere* **82**, 113-133.
**Sroczynski, S.** (1979). Das optische System des Auges des Flußbarsches (*Perca fluviatilis* L.). *Zool. Jahrb. Abt. Allg. Zool. Physiol. Tiere* **83**, 224-252.
**Sroczynski, S.** (1981). Optical system of the eye of the Ruff (*Acerina cernua* L.). *Zool. Jahrb. Abt. Allg. Zool. Physiol. Tiere* **85**, 316-342.
**Ströer, W. F. H.** (1940). Zur vergleichenden Anatomie des primären optischen Systems bei Wirbeltieren. *Z. Anat. Entwicklungsgesch.* **110**, 301-321.
**Verrier, M.-L.** (1927). Sur la structure de l'oeil de *Ameriurus nebulosus* Lesueur. et de *Clarias batrachus* L. ses rapports avec l'habitat et le comportement biologique de ces deux Siluridés. *Bull. Soc. Zool. Franc. Belg.* **52**, 581-588.
**Verrier, M.-L.** (1928). Recherches sur les yeux et la vision des poissons. *Bull. Biol. France et Belgique* **11 Suppl.**, 1-222.
**Wagner, H. J.** (1970). Der bau der Retina und der Multiple Optischen Papillae bei zwei Synodontid-Arten (Telesotei, Siluroidea). *Z. Morphol. Tiere* **68**, 69-82.
**Wagner, H.-J., Menzes, N. A. and Ali, M. A.** (1976). Retinal adaptations in some Brazilian tide pool fishes (Teleosti). *Zoomorphologie* **82**, 209-226.
**Walls, G. L.** (1963). *The Vertebrate Eye and its Adaptive Radiation*. New York: Hafner Publishing Co.
**Young, J. Z.** (1933). Comparative studies of the physiology of the iris. I. Selachians. *Proc. R. Soc. Lond. B Biol. Sci.* **112**, 228-241.